Internal Tide Energy Transfer by Nonlinear Refraction

Scott Wunsch and Theo Drivas

The Johns Hopkins University
Baltimore, Maryland, USA
scott.wunsch@jhuapl.edu

Abstract

Weakly nonlinear theory is used to explore the dynamics of a mode-1 internal tide in variable stratification. Nonlinear refraction of the internal tide at the pycnocline generates a perturbation which is forced with double the original frequency and wavenumber. The dynamics of the perturbation are analogous to a forced harmonic oscillator, with the steady state solution matching the forcing frequency and wavenumber. The perturbation exhibits resonance when its frequency is close to a natural frequency of the system. Enhanced dissipation due to the harmonic occurs near resonance, and its contribution to ocean tidal dissipation may be significant in some environments.

1 Introduction

Internal waves are ubiquitous in Earth's oceans, and a broad spectrum of internal wave frequencies and wavenumbers is observed [1, 2, 3]. Most of their power, about 1 terawatt globally, is found in low-frequency, low mode (long wavelength) internal tides [4]. Their dissipation contributes substantially to ocean mixing [5]. The geographic and vertical distribution of internal tide dissipation has a significant impact on the mixing and thermal structure of the ocean, and incomplete understanding of dissipation contributes to errors in climate prediction [6]. Multiple mechanisms have been proposed to explain the dissipation of the internal tides. Among these are scattering to smaller scale internal waves by topography [7, 8], interaction with mesoscale flow structures [9], shoaling on sloping continental shelves [10], and parametric subharmonic instability [11, 12], although recent observations suggest the latter is not relevant for mode-1 diurnal tides [13]. It is plausible that no single dissipation mechanism is globally dominant, but instead that the relative importance of different mechanisms varies geographically and seasonally.

There has been much recent progress in understanding the nonlinear mechanisms which transfer internal wave energy to smaller scales. One prominent example is the excitation of double-frequency and -wavenumber harmonics by refraction of a single mode. The harmonic effect was first observed for internal wave beams propagating through sharply increasing stratification by [14, 15] using numerical simulations, and quickly followed in the laboratory [16, 17]. Additional numerical studies also observed the effect [18, 19]. Although the connection between harmonics and variable stratification was not immediately recognized, the subsequent weakly nonlinear theory of [20] clearly derived the connection between variable stratification and harmonic generation by a single mode. For beams, the relative importance of nonlinear refraction of a single mode and wave-wave interactions (which generally give rise to double-frequency, but not double-wavenumber harmonics) was further investigated by [21, 22]. Initial transients produced by single mode internal waves have recently been investigated by [23].

The generation of double-frequency harmonics by oceanic internal tides has also been observed in the South China Sea by [24], who immediately recognized the connection

to the laboratory observations of [16]. The harmonic mode is transient, appearing and disappearing from the observed currents over periods of several days. The subsequent calculation of the expected steady-state harmonic amplitude by [25], using the weakly nonlinear theory of [20], demonstrated that variable stratification was plausibly the cause of the observed harmonic. The steady-state amplitude depends strongly on the pycnocline characteristics, suggesting that gradual changes in the stratification profile might be responsible for the transient nature of the observations. Double-frequency harmonics have also been observed in numerical simulations of internal tides by [7], who noted that the harmonics only occurred when variable stratification was used.

2 Weakly nonlinear theory

Here, the weakly nonlinear theory of single-mode internal wave refraction developed in [20, 22, 25] for steady-state harmonics is extended to include transients and dissipation. The effect of rotation is neglected. The results are used to explore the possible role nonlinear refraction might play in the dissipation of the oceanic internal tides. Utilizing weakly nonlinear theory (rather than full numerical simulations) permits a much more complete exploration of the parameter space. Using the theoretical framework for a two dimensional Bousinesq fluid [26] [27] with buoyancy frequency $N(z)$, the stream function $\psi(x,z,t)$ ($u \equiv \partial_z\psi$, $w \equiv -\partial_x\psi$) is decomposed into a single primary mode ψ_o, with frequency ω and horizontal wavenumber k, and a (smaller amplitude) perturbation $\delta\psi$, as

$$\psi\left(x,z,t\right) = A_o\psi_o\left(z\right)e^{i(kx-\omega t)} + \delta\psi\left(x,z,t\right) + c.c \tag{1}$$

where A_o represents the dimensionless amplitude of the primary mode and $c.c$ denotes complex conjugate (so that the solutions are real). The primary mode obeys the linear equation [28]

$$\partial_z^2\psi_o + k^2\left(\left(\frac{N}{\omega}\right)^2 - 1\right)\psi_o = \frac{i\nu}{\omega}\left(\partial_z^2 - k^2\right)^2\psi_o \tag{2}$$

The perturbation, to lowest order, obeys

$$\partial_t^2\nabla^2\delta\psi + N^2\partial_x^2\delta\psi - \nu\nabla^4\partial_t\delta\psi = -\frac{4k^3}{\omega}\left(\partial_z N^2\right)\psi_o^2 e^{2i(kx-\omega t)} \tag{3}$$

In uniform stratification N, there is no forcing for $\delta\psi$ and the primary mode is an exact solution [27]. Equation (3) shows that internal wave refraction through any vertically-varying stratification profile (non-zero $\partial_z N^2$) generates harmonic modes, as first suggested by [20]. Mathematically, Eq. (3) is analogous to a system of forced simple harmonic oscillators, and its solutions can be written approximately in terms of eigenmodes ψ_n with natural frequencies ω_n as

$$\delta\psi\left(x,z,t\right) = \psi_h(z)e^{2i(kx-\omega t)} + \sum_n A_n\psi_n(z)e^{i(2kx-\omega_n t)} \tag{4}$$

where ψ_h represents the steady-state harmonic solution, which obeys the equation previously derived by [20] for $\nu = 0$. The homogeneous (unforced) solutions of the same equation are normalized to satisfy orthonormality and the constants A_n are chosen to match the initial conditions. Like a forced harmonic oscillator, transient modes in Eq. 4

gradually decay, ultimately leaving the steady-state solution $\delta\psi = \psi_h$. The time required for ψ_h to emerge depends on the proximity of the forcing to a homogeneous solution, often referred to as the degree of resonance, along with the magnitude of the damping (ν) in the system. Hence the relationship between the forcing frequency ω and the spectrum of natural eigenfrequencies $\omega_n(2k)$ at the harmonic wavenumber $2k$ is vital to understanding the dynamics of the system.

With nonzero viscosity, the eigenmode expansion in Eq. 4 is only approximate. In this analysis, viscous effects are assumed to be small and are only retained in the time dependence of the modes, while inviscid spatial solutions represent the vertical structure. With this approximation, the unforced terms in Eq. 4 decay, ultimately leaving the steady-state solution with a frequency 2ω and wavenumber $2k$.

3 Results

In general, numerical methods are needed to solve Equation (3) for an arbitrary stratification profile $N(z)$. To explore the solution characteristics analytically, an idealized stratification profile with piecewise-constant $N(z)$ is used here. This approach generalizes the work of [28] to the weakly nonlinear regime, and was used previously to establish the connection between variable stratification and harmonic generation for plane internal waves [20, 21] and single-mode internal tides [25]. The stratification $N(z)$ is constant except for a thin pycnocline and mixed layer at the top:

$$N(z) = \left\{ \begin{array}{cc} 0 & -h+\delta < z < 0 \\ N_p & -h < z < -h+\delta \\ N_o & -H < z < -h \end{array} \right) \tag{5}$$

The profile is representative of realistic ocean profiles for $\delta < h \ll H$, but also reduces to the "top-hat" profile (larger δ and $N_p \gg N_o$) which has also been used to explore harmonic generation [23]. Solutions of Eq. 2 for the primary mode ψ_o are found using the boundary conditions $\psi = 0$ at $z = [-H, 0]$ and matching conditions at the layer boundaries, as in [28, 20, 25]. The result is

$$\psi_o = A_o \left\{ \begin{array}{cc} a\sinh(kz) & -h+\delta < z < 0 \\ b\sin(q_p z) + c\cos(q_p z) & -h < z < -h+\delta \\ d\sin(q(H+z)) & -H < z < -h \end{array} \right. \tag{6}$$

where A_o is the steady state amplitude of the mode and the constants a, b, c, d are determined by the matching conditions. The frequency ω is given by

$$\frac{\omega}{N_o} \simeq \frac{\pm k}{\sqrt{k^2+q^2}} - \frac{i\nu}{2N_o}\left(k^2+q^2\right) \tag{7}$$

where the imaginary term determines the viscous decay rate of the mode. For a non-zero amplitude, the matching conditions require that q and q_p satisfy the dispersion relation

$$q_p \tan(q(H-h)) = -q\tan(q_p\delta + \chi) \tag{8}$$

$$q_p = k\sqrt{\left(\frac{N_p}{N_o}\right)^2\left(1+\frac{q^2}{k^2}\right) - 1} \tag{9}$$

$$\tan\chi \equiv \frac{q_p}{k}\tanh k\,(h-\delta) \tag{10}$$

In the limit $\delta \to 0$, this reduces to the dispersion relation found in [22]. Equation (10) is solved numerically to find the allowed values of q as a function of k. This yields a spectrum of eigenmodes ψ_n, one of which is selected as the dominant mode ψ_o.

The orthonormal basis functions for the harmonic solution $\delta\psi$ are computed in the same manner, except with double the wavenumber of the primary mode ($k \to 2k$). The steady-state harmonic solution ψ_s is found by substitution into Equation 3:

$$\psi_h = A_h \begin{cases} a_h \sinh(2kz) & -h+\delta < z < 0 \\ b_h \sin(2q'_p z) + c_h \cos(2q'_p z) & -h < z < -h+\delta \\ d_h \sin(2q'(H+z)) & -H < z < -h \end{cases} \tag{11}$$

$$q'^2 = k^2 \left(\frac{N_o^2}{4\omega^2} - 1 \right), \quad q'^2_p = k^2 \left(\frac{N_p^2}{4\omega^2} - 1 \right) \tag{12}$$

where k and ω are the wavenumber and frequency of the primary (forcing) mode. The amplitude A_h is determined by the primary mode amplitude and is proportional to the square of the primary mode amplitude, as is typical for weakly nonlinear phenomena. The full expression for A_h is cumbersome and not very enlightening, and so is omitted for brevity. Like the thin pycnocline limit ($\delta \to 0$) computed by [25], the denominator of the expression contains the dispersion relation, and vanishes if the forcing frequency 2ω lies near one of the natural modes ω_n. This resonance criterion determines the conditions under which a strong harmonic response to forcing by the primary mode is expected.

Figure 1 presents an example of the temporal development of the perturbation to a mode-1 internal tide for conditions which are comparable to the South China Sea observations of [24]. The water depth H is 2500 m, the pycnocline depth h is 75 m and its thickness δ is 25 m, and the dimensionless density change across the pycnocline [25] is $g\Delta\rho/\rho N_o^2 H = 2$. The dimensionless amplitude of the primary mode $A_o = 0.005$, which was selected to yield horizontal currents of ~ 0.3 m/s, as in [24]. The eddy diffusivity is $\nu \sim 0.5$ m^2/s, which is on the low end of estimates for the ocean [29]. Larger values of ν would more rapidly damp out transients, causing the steady state solution to emerge more quickly. The example shows the perturbation initially emerging near the pycnocline, as expected since this is where the gradients in $N(z)$ are found. After a few periods, it grows and takes the form of the steady state mode, but does not reach full amplitude for tens of periods, which is longer than the typical duration of the harmonic mode (~ 10 periods) observed in [24]. The emergence of the steady state harmonic mode is more rapid when the system is near resonance, and very slow when far from resonance.

Of greater interest for oceanographic applications is the potential enhancement of the dissipation rate ϵ in various environments due to nonlinear refraction. This is explored in Figure 2 as a function of pycnocline depth h/H and the density change across the pycnocline. Here, the pycnocline thickness is fixed at $\delta = 0.01H$. The added dissipation due to the harmonic ϵ_H is normalized by the dissipation rate of the primary mode, $\epsilon_H/A_o^2\epsilon_o$, and is shown on a logarithmic (base 10) color scale. Due to the nonlinear nature of the perturbation, it is also proportional to the primary mode amplitude A_o^2, which is $\sim 3\cdot 10^{-5}$ for the South China Sea example. After only a few periods (left panel), there is a substantial increase in dissipation only in the vicinity of resonance (red curve). Substantially enhanced dissipation covers a much broader part of parameter space in the steady state. In the South China Sea example, the estimated value of ϵ_o due to the primary mode

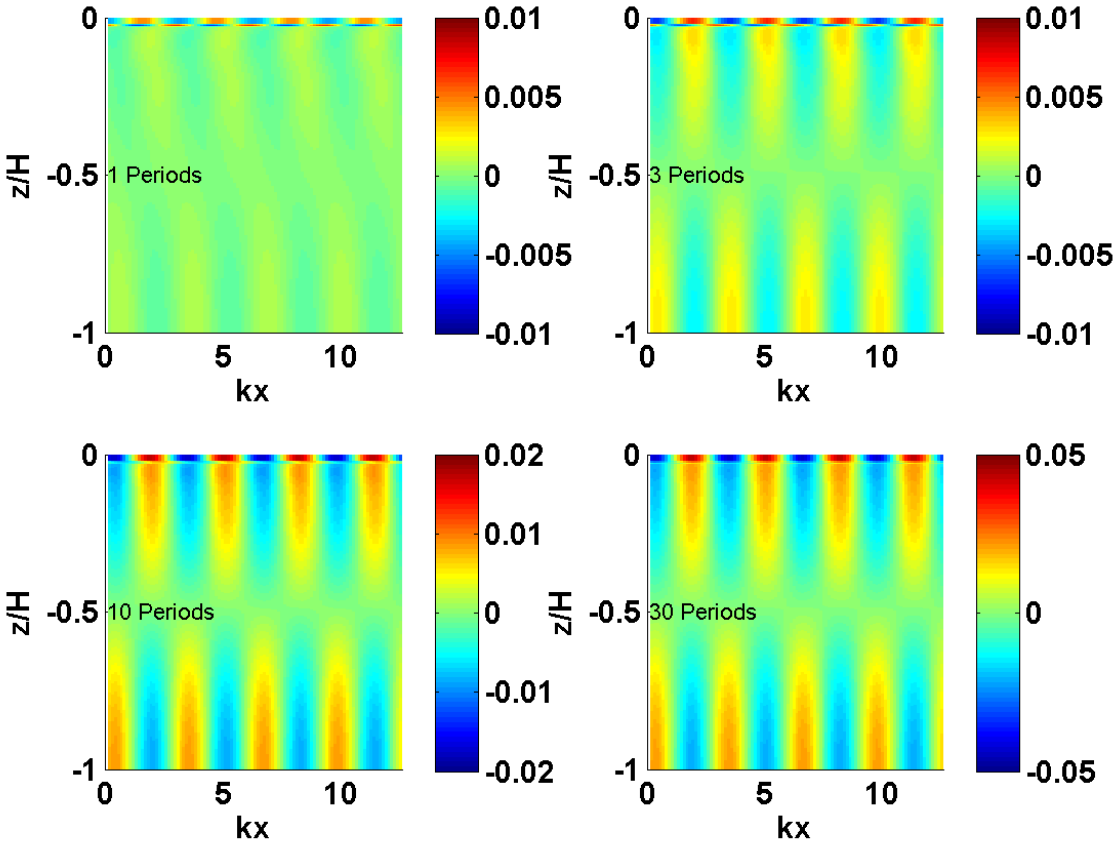

Figure 1: Growth of the harmonic mode horizontal current, after $1 - 30$ periods of the primary mode. Color bar is in m/s. Primary mode current is ~ 0.3 m/s, and other parameters are representative of South China Sea observations of [24].

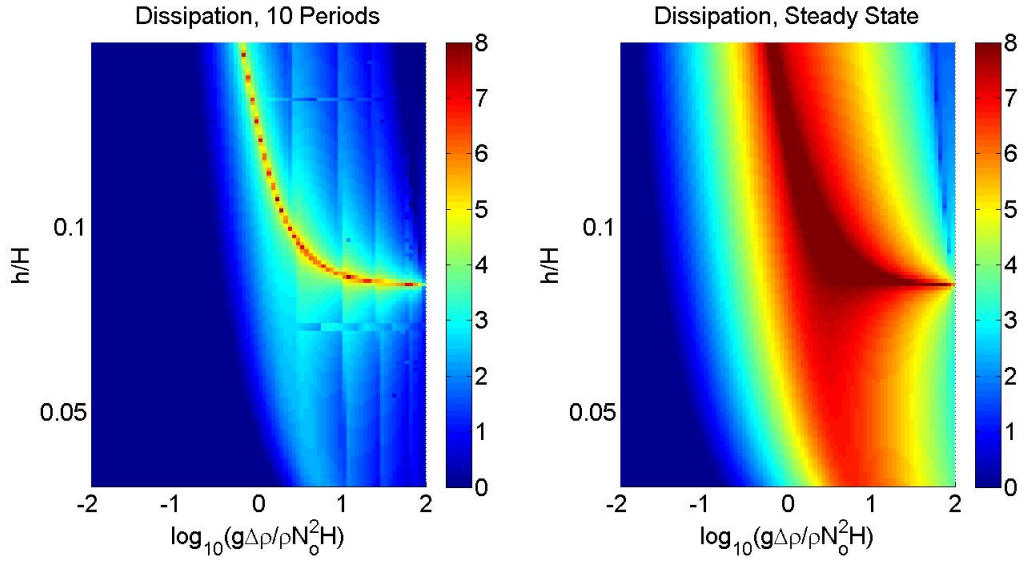

Figure 2: The increase in dissipation rate $log_{10}(\epsilon_H / A_o^2 \epsilon_o)$ due to nonlinear refraction, normalized by the primary mode dissipation rate.

would be $\sim 10^{-10}$ m^{2}s^{-3}, which is much less than the global average of $\sim 10^{-9}$ m^{2}s^{-3} (1 Terrawatt divided by 10^{21} kg in the global oceans). In the example of Figure 2, for $A_o^2 \sim 3 \cdot 10^{-5}$, those regions with $\epsilon_H / A_o^2 \epsilon_o > 10^4$ (green/yellow) have dissipation rates which are significantly increased by the harmonic, and those with $\epsilon_H / A_o^2 \epsilon_o > 10^5$ (red) have dissipation rates which significantly exceed the global average. This example indicates that, for realistic ocean conditions, nonlinear refraction could significantly increase tidal dissipation in some environments, but that in many other cases the effect would be negligible.

4 Discussion

These results illustrate the dynamics of nonlinear refraction for the generation of harmonic perturbations to internal tides. Analogous to a forced harmonic oscillator, resonance between the forcing frequency and the natural modes of the system is critical to the dynamics. Near-resonant systems exhibit a strong response, and the steady state solution emerges relatively rapidly. Non-resonant systems have a weaker response and are slower to reach the steady state. The approach captures the essence of the dynamics reported for the fully nonlinear simulations reported by [23], which finds rapid emergence of the steady state for ocean-like stratifications (near resonance) but not for "top-hat" profiles (non-resonant).

Weakly nonlinear theory with an idealized ocean stratification profile has been used here to estimate the possible contribution of nonlinear refraction to the dissipation in oceanic internal tides. The results show that, in near-resonant conditions, significant enhancement of dissipation may occur, but that in non-resonant conditions the effect is not important. Geographic and seasonal variations in dissipation would therefore be expected. Changing conditions could cause harmonics to grow and decay, as in the observations of [24].

In future work, rotation must be added to the analysis to accurately represent ocean conditions at higher latitudes. It should also be straightforward to extend the approach to arbitrary stratification profiles by computing eigenmodes numerically. This would permit calculation of resonance conditions and the likelihood of observing strong nonlinear refraction for real ocean stratification profiles. Such results could guide future observations as well as assess the possible contribution of nonlinear refraction to the global dissipation of internal tides.

References

[1] Garrett, C. and Munk. W., Internal waves in the ocean. *Ann. Rev. Fluid Mech.* **11**, 339-369 (1979).

[2] Holloway, G., Oceanic internal waves are not weak waves. *J. Phys. Oceanogr.* **10**, 906914 (1980).

[3] Garrett, C., Internal tides and ocean mixing. *Science* **308**, 1858-59 (2003).

[4] Munk, W. and Wunsch, C., Abyssal recipes II: energetics of tidal and wind mixing. *Deep-Sea Res. I* **45**, 1977-2010 (1998).

[5] Garrett, C. and Kunze, E., Internal tide generation in the deep ocean. *Ann. Rev. Fluid Mech.* **39**, 57-87 (2007).

[6] Melet, A., Hallberg, R., Legg, S., and Polzin, K., Sensitivity of the Ocean state to the vertical distribution of internal-tide-driven mixing. *J. Phys. Oceanogr.* **43**, 602-615 (2013).

[7] Johnston, T.M.S., and Merrifield, M.A., Internal tide scattering at seamounts, ridges, and islands. *J. Geophys. Res.* **108**, 3180 (2003).

[8] Balmforth, N. J., and Peacock, T., Tidal conversion by supercritical topography. *J. Phys. Oceanogr.* **39**, 19651974 (2009).

[9] Rainville, L. and Pinkel, R., Propagation of low-mode internal waves through the ocean. *J. Phys. Oceanogr.* **36**, 12201236 (2006).

[10] Kunze, E., and Llewellyn-Smith, S.G., The role of small-scale topography in turbulent mixing of the global ocean. *Oceanography* **17**, 55-64 (2004).

[11] MacKinnon, J.A., and K.B. Winters, K.B., Subtropical catastrophe: significant loss of low-mode tidal energy at 28.9 degrees. *Geophys. Res. Lett.* **32** L15605 (2005).

[12] Xie, X., Chen, G., Shang, X., and Fang, W., Evolution of the semidiurnal (M_2) internal tide on the continental slope for the northern South China Sea. *Geophys. Res. Lett.* **35**, L13604 (2008).

[13] Zhao, Z., Alford, M.H., Girton, J.B., Rainville, L., and Simmons, H. Global observations of open-ocean Mode-1 M_2 internal tides. *J. Phys. Oceanogr.* **46**, 1657-1683 (2016).

[14] Grisouard N., and Staquet, C., Numerical simulations of the local generation of internal solitary waves in the Bay of Biscay. *Nonlin. Processes Geophys.* **17**, 575584 (2010).

[15] Grisouard, N., Staquet, C., and Gerkema, T. Generation of internal solitary waves in a pycnocline by an internal wave beam: a numerical study. *J. Fluid Mech.* **676**, 491-513 (2011).

[16] Mercier, M.J., Mathur, M., Gostiaux, L., Gerkema, T., Magalhaes, J.M., da Silva, J.C.B. and Dauxois, T., Soliton generation by internal tidal beams impinging on a pycnocline: laboratory experiments. *J. Fluid Mech.* **704**, 37-60 (2012).

[17] Wunsch, S., and Brandt, A., Laboratory experiments on internal wave interactions with a pycnocline. *Exp. Fluids* **53**, 1663-1679 (2012).

[18] Gayen, B., and Sarkar, S., Degradation of an internal wave beam by parametric subharmonic instability in an upper ocean pycnocline. *J. Geophys. Res. Oceans* **118** (2013).

[19] Dossmann, Y., Auclair, F., and Paci, A., Topographically induced internal solitary waves in a pycnocline: Secondary generation and selection criteria. *Phys. Fluids* **25**, 086603 (2013).

[20] Diamessis, P.J., Wunsch, S., Delwiche, I., and Richter, M.P., Nonlinear generation of harmonics through the interaction of an internal wave beam with a model oceanic pycnocline. *Dyn. Atmos. Oceans* **66**, 110-137 (2014).

[21] Wunsch, S., Ku, H., Delwiche, I., and Awadallah, R., Simulations of nonlinear harmonic generation by an internal wave beam incident on a pycnocline. *Nonlin. Processes. Geophys.* **21**, 855-868 (2014).

[22] Wunsch, S., Delwiche, I., Frederick, G., and Brandt, A., Experimental study of nonlinear harmonic generation by internal waves incident on a pycnocline. *Exp. Fluids* **56**:87 (2015).

[23] Sutherland, B.R., Excitation of superharmonics by internal modes in non-uniformly stratifed fluid. *J. Fluid Mech.* **793**, 335-352 (2016).

[24] Xie, X., Shang, X., van Haren, H., and Chen, G., Observations of enhanced nonlinear instability in the surface reflection of internal tides. *Geophys. Res. Lett.* **40**, 1580-1586 (2013).

[25] Wunsch, S., Nonlinear harmonic generation by diurnal tides. *Dyn. Atmos. Oceans* **71**, 91-97 (2015).

[26] Tabaei, A., and Akylas, T.R., Nonlinear internal gravity beams. *J. Fluid Mech.* **482**, 141-161 (2003).

[27] Tabaei, A., Akylas, T.R., and Lamb, K.G., Nonlinear effects in reflecting and colliding internal wave beams. *J. Fluid Mech.* **526**, 217-243 (2005).

[28] Mathur, M., and Peacock, T., Internal wave propagation in non-uniform stratifications. *J. Fluid Mech.* **639**, 133-152 (2009).

[29] Marshall, J., Shuckburgh, E., Jones, H., and Hill, C. Estimates of implications of surface eddy diffusivity in the Southern Ocean derived from tracer transport. *J. Phys. Oceanogr.* **36**, 1806-1821 (2010).